Wave excitation by nonlinear coupling among shear Alfvén waves in a mirror-confined plasma

R. Ikezoe, M. Ichimura, T. Okada, M. Hirata, T. Yokoyama, Y. Iwamoto, S. Sumida, S. Jang, K. Takeyama, M. Yoshikawa, J. Kohagura, Y. Shima, and X. Wang

Citation: Physics of Plasmas **22**, 090701 (2015); doi: 10.1063/1.4930216
View online: http://dx.doi.org/10.1063/1.4930216
View Table of Contents: http://scitation.aip.org/content/aip/journal/pop/22/9?ver=pdfcov
Published by the AIP Publishing

Wave excitation by nonlinear coupling among shear Alfvén waves in a mirror-confined plasma

R. Ikezoe,[a] M. Ichimura, T. Okada, M. Hirata, T. Yokoyama, Y. Iwamoto, S. Sumida, S. Jang, K. Takeyama, M. Yoshikawa, J. Kohagura, Y. Shima, and X. Wang
Plasma Research Center, University of Tsukuba, Tsukuba 305-8577, Japan

(Received 23 March 2015; accepted 20 August 2015; published online 2 September 2015)

A shear Alfvén wave at slightly below the ion-cyclotron frequency overcomes the ion-cyclotron damping and grows because of the strong anisotropy of the ion temperature in the magnetic mirror configuration, and is called the Alfvén ion-cyclotron (AIC) wave. Density fluctuations caused by the AIC waves and the ion-cyclotron range of frequencies (ICRF) waves used for ion heating have been detected using a reflectometer in a wide radial region of the GAMMA 10 tandem mirror plasma. Various wave-wave couplings are clearly observed in the density fluctuations in the interior of the plasma, but these couplings are not so clear in the magnetic fluctuations at the plasma edge when measured using a pick-up coil. A radial dependence of the nonlinearity is found, particularly in waves with the difference frequencies of the AIC waves; bispectral analysis shows that such wave-wave coupling is significant near the core, but is not so evident at the periphery. In contrast, nonlinear coupling with the low-frequency background turbulence is quite distinct at the periphery. Nonlinear coupling associated with the AIC waves may play a significant role in the beta- and anisotropy-limits of a mirror-confined plasma through decay of the ICRF heating power and degradation of the plasma confinement by nonlinearly generated waves.
 [http://dx.doi.org/10.1063/1.4930216]

Many types of nonlinear phenomena exist in magnetized plasmas in fusion experiments. These phenomena frequently play crucial roles in processes such as the self-organization and sustainment of the global structure, relaxation processes, and saturation mechanisms.[1–5] In the case of radiofrequency plasma heating, nonlinear phenomena play a major role in the heating efficiency; for example, parametric instability is a major concern in fusion research and the problem has been actively researched.[6,7] In the GAMMA 10 tandem mirror,[8,9] plasma is generated and heated by the ion-cyclotron range of frequencies (ICRF) waves. The confined ion energy in the main confinement region (called the central cell) saturates after Alfvén ion-cyclotron (AIC) waves are spontaneously excited because of strong ion-temperature anisotropy.[10] The precise excitation threshold is discussed in Ref. 10. The theoretical approach, in which the finite axial distribution of the high beta and anisotropic region in the central cell is considered, shows good agreement with experimental results. Because there is a strong correlation between the excitation of the AIC waves and the saturation of the confined energy, the AIC waves must play some key role, either directly or indirectly, in the beta-limit of mirror-confined plasmas. Interaction between the AIC wave and the ICRF waves for heating would be one saturation mechanism that leads to the decay of the ICRF heating power. Also, interactions between each of the AIC waves would be another saturation mechanism that could lead to enhancement of the ion loss produced by low-frequency waves generated through such interactions. Coincident occurrence of this saturation and the emergence of nonlinear coupling are reported in Ref. 11, along with an observation of the axial transport of high-energy ions that shows burst-like behavior with the difference frequencies of the AIC waves rather than steady behavior. Therefore, these waves are likely to interact with the high-energy ions that bounce in the mirror field and cause pitch angle scattering to push the ions into the loss cone. In this paper, clear evidence of nonlinear coupling between the AIC and ICRF waves and the radially localized nonlinear generation of these waves with the difference frequencies of the AIC waves is shown by applying a bispectral analysis to the density fluctuation signals that were obtained over a wide radial region in GAMMA 10 using a reflectometer.

The waves that are treated in this study are a slow wave for magnetic beach heating at 6.36 MHz (where the resonance is located near the midplane of the central cell), spontaneously excited slow waves (AIC waves) at 5.6–5.9 MHz (slightly below the ion-cyclotron frequency at the midplane), and nonlinearly excited waves. The characteristics of a typical plasma that are produced solely by ICRF waves in GAMMA 10 can be found in Ref. 12, where the base plasma is generated using fast waves at 9.9 and 10.3 MHz from Nagoya type-III antennas with hydrogen gas injection into the hydrogen seed plasma produced by plasma guns. Acceleration of the electrons by Landau damping and the oscillating near-field of the Nagoya type-III antennas both affect the plasma production. These fast waves are also mode-converted into slow waves between the central cell and subsequent anchor cells and are absorbed by the ions in the anchor cells,[13] which offers magnetohydrodynamic (MHD) stability to the entire plasma because of the minimum-B configuration.[14] The operational regime that was recently extended for the

[a]Email: ikezoe@prc.tsukuba.ac.jp

ongoing divertor simulation experiment in GAMMA 10/PDX is presented in Ref. 15.

A reflectometer, which we use for wave detection, is a useful tool for investigation of the density fluctuation behavior that occurs inside hot plasma while using a relatively small-sized measurement system. Reflectometers have been applied to many fusion plasma experiments, with interests in many topics.[16–27] In this study, we use a reflectometer to detect the relatively large-scale structures related to waves in the ICRF in a cylindrical plasma, where those excitations are severely restricted by the boundary conditions. The global wave-field structure that satisfies the boundary conditions can only grow if the wavelength is comparable to the machine size; this is the case for these ICRF waves, including the AIC waves, in GAMMA 10. Electromagnetic waves in the ICRF are theoretically shown to accompany the corresponding density fluctuations.[28,29] It was shown by comparison of the X- and O-mode reflectometer signals that the magnetic fluctuation level of the AIC waves is of the order of 10^{-4}, and the level of the accompanying density fluctuations is comparable to that level.[17] Because the structure has such a small amplitude and a long wavelength, the phase modulation $\tilde{\varphi}$ can be estimated well using one-dimensional geometric optics and gives $\tilde{\varphi} \ll 1$ rad for both the ICRF and AIC waves. Therefore, reflectometry would work well for the intended application. There have been previous successful demonstrations of ICRF wave detection by reflectometry.[18,19]

O-mode microwaves in the frequency range from 8 to 12 GHz are used as the probing microwave signal. The radial density profile of the GAMMA 10 plasma is a monotonically decreasing function of the radius and it is maintained almost constantly, except for discharges using abnormal amounts of gas injection or other additional heatings, such as electron cyclotron heating (ECH) and neutral beam injection (NBI). In this case, the density profile is closely related to the formed eigenmode of the ICRF waves,[30] which does not vary much within the normal ICRF power range. The measurement position (i.e., the cutoff position) in this study covers a wide radial region; $r/a \sim 0.8$, 0.7, 0.6, 0.5, and 0.3 for O-mode microwave frequencies of 8, 9, 10, 11, and 12 GHz, respectively, where r and a are the radius and the plasma radius of the GAMMA 10 central cell ($a = 0.18$ m), respectively.

A density fluctuation measured using an 11 GHz probing frequency at $z = 1.12$ m is compared with a magnetic fluctuation that was measured at the edge of the same cross-section, as shown in Fig. 1; $z = 0$ is set on the midplane of the central cell, and the axial location of the central cell is from $z = -2.8$ m to $z = 2.8$ m. Peaks at 6.36, 9.9, and 10.3 MHz correspond to the externally applied ICRF waves, and several peaks seen in the 5.6–5.9 MHz range are associated with the AIC waves. As the frequency spectrum of the density fluctuation clearly shows several peaks appear at the sum and difference frequencies of the 6.36 MHz wave and the AIC peak frequencies, and peaks also appear around the second harmonic frequencies of the AIC waves, whereas these peaks are not so clear in the edge magnetic fluctuation. If we adequately amplify the signal and apply some filtering, we can also see these peaks in the magnetic fluctuation.

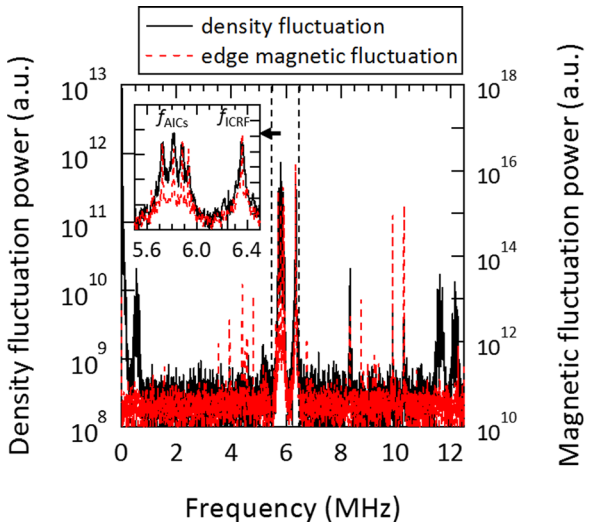

FIG. 1. Comparison of the density fluctuation power spectra measured by a reflectometer and the magnetic fluctuation measured at the edge by a pick-up coil on the same cross-section at $z = 1.12$ m.

However, Fig. 1 distinctly demonstrates the advantage of using a reflectometer to investigate these nonlinear phenomena in GAMMA 10 when compared with the commonly used pick-up coil that is set at the periphery. This difference can be explained by the measurement position, i.e., the position inside or just outside the plasma. Wavenumber matching for the waves at the difference frequencies of the 6.36 MHz wave and the AIC frequencies was previously confirmed using edge pick-up coils, although the results were not so clear because of the existence of the resonance of the 6.36 MHz slow wave and because of difficulties encountered in the detection of the nonlinearly excited waves that emerged inside the plasma, as described above.[31] By using the advantages of the reflectometer and by also applying a bispectral analysis, we evaluate the nonlinear coupling inside the plasma in the following. Note that this study is limited to the frequency space, and thus the wavenumber space is not included. Detection of the appropriate wavenumbers in the plasma region using a two-channel reflectometer is currently under investigation.

For nonlinear coupling of the three-wave interaction, the wave frequencies and wavenumbers must satisfy the appropriate matching conditions: $f_1 + f_2 = f_3$ and $k_1 + k_2 = k_3$. Also, a constant phase relationship must hold among the three interacting waves; otherwise, they are simply independently excited waves, even if the waves do satisfy the matching condition. When determining whether the waves are independent or nonlinearly coupled, bispectral analysis is useful (see, e.g., Refs. 5, 32, and 33). The squared bicoherence is defined by $b^2(k,l) = \mathrm{E}[\boldsymbol{X}_k\ \boldsymbol{X}_l\ \boldsymbol{X}_{k+l}^*]/(\mathrm{E}[|\boldsymbol{X}_k\ \boldsymbol{X}_l|^2]\mathrm{E}[|\boldsymbol{X}_{k+l}|^2])$, where E is the expectation operator and $\boldsymbol{X}_k$ is the complex Fourier amplitude of the frequency or the wavenumber of k. A statistically meaningful calculation of the bicoherence requires appropriate treatment of the expectation operator. The variance is reduced by a factor of $1/M$, where M is the averaging number. We collect each ensemble from the steady state in three identical discharges. The total for M for the following calculations is approximately 900.

The calculated squared bicoherence for the dataset that was obtained using 11 GHz microwave probing is shown in Fig. 2, with the frequency region expanded around the sum and difference interactions between the 6.36 MHz ICRF wave and the AIC waves. The frequency spectra that were averaged over the same ensembles with those used for calculation of the squared bicoherence are shown in Figs. 2(a) and 3. The large peaks that were attributed to three AIC waves are found in this dataset. At the sum and difference frequencies between the 6.36 MHz wave and the AIC frequencies, the squared bicoherence remains high after adequate ensemble averaging. These values lie well above the statistical noise level, and they produce the waves at the sum and difference frequencies that are observed in the spectra shown in Fig. 3. These interactions should partly contribute to the observed saturation of the confined energy; a proportion of the ICRF heating power is delivered to the nonlinearly excited waves through coupling with the AIC waves. In Fig. 3, round peaks are also observed around the second harmonic of the AIC waves in the 11.4–11.8 MHz range. Because there are several possible combinations among the three AIC waves, as indicated by the calculated bicoherence shown in Fig. 2(b), the spectrum has relatively

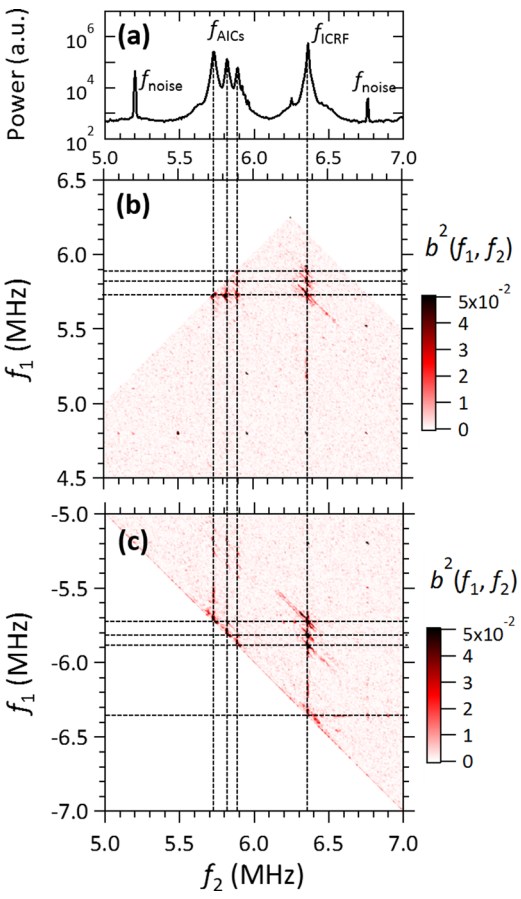

FIG. 2. (a) Ensemble-averaged power spectrum of the density fluctuation as measured by a reflectometer using 11 GHz O-mode microwaves and the squared bicoherence of (b) the sum and (c) the difference interactions between externally applied ICRF waves and spontaneously excited AIC waves. The calculation region is limited by the Nyquist frequency, which is 12.5 MHz in this dataset, and the symmetry of the bispectrum.

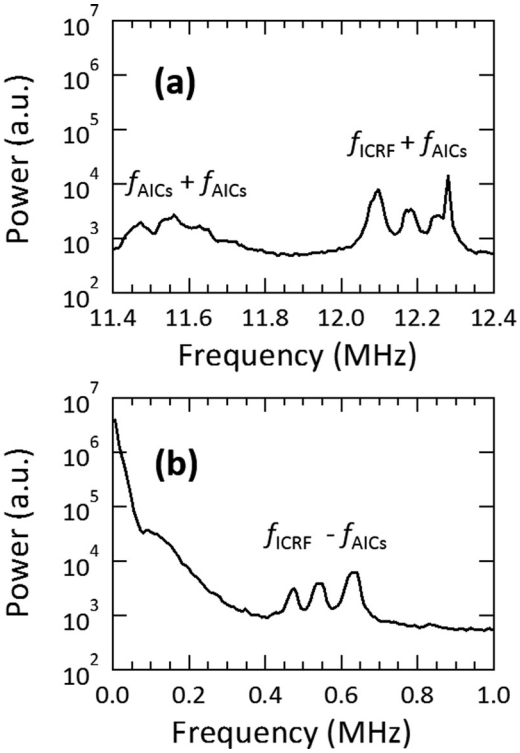

FIG. 3. Ensemble-averaged power spectra of the density fluctuations measured using a reflectometer with 11 GHz O-mode microwaves in the frequency ranges of (a) 11.4–12.4 MHz and (b) 0–1.0 MHz.

complex round peaks caused by the superposition of each corresponding peak.

Next, we demonstrate the nonlinear excitation of the low-frequency waves with the difference frequencies of the AIC waves, which is related to axial transport of high-energy ions, as mentioned earlier. Figure 4 shows a comparison of the squared bicoherence of the different datasets that were obtained near the core ($f_{probing} = 12$ GHz) and at the periphery ($f_{probing} = 9$ GHz). This figure focuses on the difference interaction between the AIC waves. To indicate the frequencies of the AIC waves, the ensemble-averaged spectra are also shown in Fig. 4(b). The small shift shown in two of the spectra can be attributed to small variations in the plasma parameters, which are hard to avoid because of changes in the uncontrollable wall conditions, although we did perform the measurements using successive discharges over a single day. However, this small frequency shift does not play any significant role in the radial dependence of the three-wave coupling that is considered here. A comparison between (a) and (c) clearly shows the radial variation of the coupling strength that generates the low-frequency waves with the difference frequencies of the AIC waves; the squared bicoherence is significant near the core (Fig. 4(a)), but less so at the periphery (Fig. 4(c)).

To state the radial dependence that is seen in Fig. 4 clearly, we summed the squared bicoherence values over all combinations of f_1 and f_2 to produce a constant f_3. This summation corresponds to an integration along the line $f_2 = -f_1 + f_3$ when f_3 is fixed. This summed squared bicoherence can indicate the degree to which the nonlinearity is included in the f_3 component, regardless of which

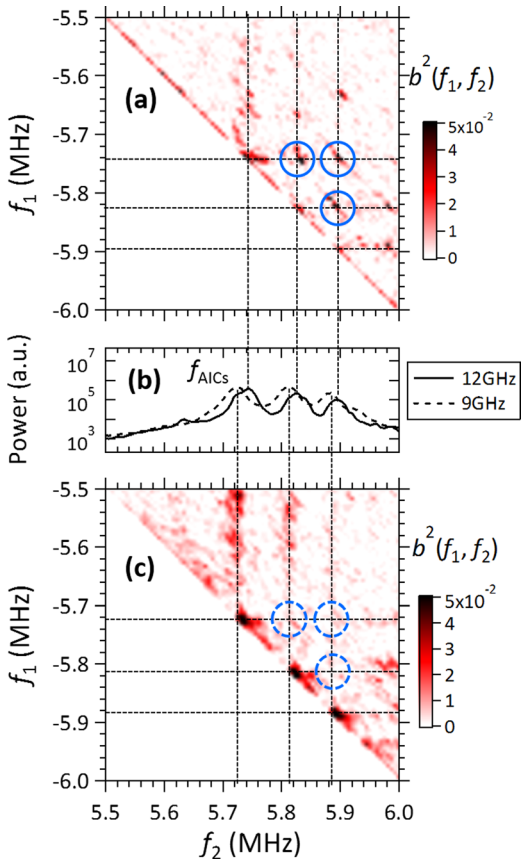

FIG. 4. Squared bicoherences showing difference interactions between the AIC waves for the datasets obtained by (a) 12 GHz (core region) and (c) 9 GHz (near periphery) microwave reflectometry, and (b) the ensemble-averaged power spectra of the corresponding density fluctuations.

combinations are particularly dominant. Figure 5 shows the summed squared bicoherence as a function of f_3 for five microwave probing frequencies. The summed squared bicoherence has peaks at around 70, 90, and 160 kHz, which are the exact difference frequencies of the AIC waves, for 12 GHz microwave probing, but the peaks are not so clear at the other probing frequencies. Because the summed squared bicoherence is also significant in the outer region for the waves that were generated via the coupling between the 6.36 MHz ICRF wave and the AIC waves, the localized nonlinear coupling that was found in the low-frequency waves may be related to the properties of the generated waves. It

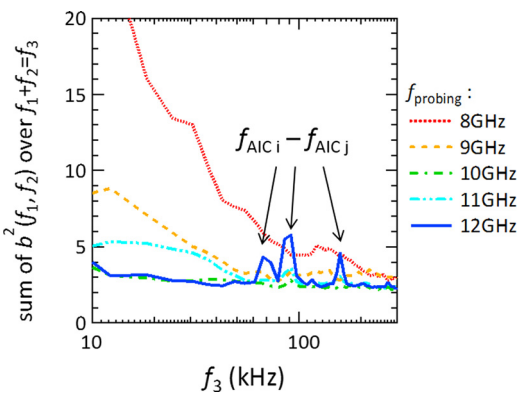

FIG. 5. Radial dependence of the summed squared bicoherence.

should be noted here that because these low-frequency waves have small wavenumbers under the matching condition $k_{AICi} - k_{AICj} = k_{lf}$, the wavelengths become longer and the geometric optics approximation of reflectometry also holds for the low-frequency waves. On the other hand, there is significant nonlinearity in the low-frequency region below 100 kHz in the peripheral region. Background plasma turbulence may be interacting and causing spectral broadening at the periphery in this case. However, a detailed evaluation is required for such a small-scale phenomenon when measured using a microwave reflectometer, because the microwave reflection shows complex behavior when influenced by small-scale turbulence. We have limited our studies to the emergence of the radial dependence here and have not attempted a precise assessment of the coupling with the small-scale turbulence, which seems to occur near the periphery.

In summary, nonlinear (three-wave) couplings among shear Alfvén waves, which are those applied for ion heating and those that are spontaneously excited because of ion-temperature anisotropy (AIC waves), and their radial dependence have been evaluated by applying a bispectral analysis to the density fluctuations that were measured using a reflectometer in GAMMA 10. The emergence of several fluctuations is explained well by three-wave coupling among the waves of which the driving forces are apparent. The strength of the three-wave coupling varies in the radial direction; the bicoherence of the coupling between the AIC waves required to produce low-frequency difference fluctuations is significant near the core region but is less significant in the outer region. This radial dependence could be attributed to the properties of the generated low-frequency waves, because another instance of coupling between the AIC waves and the ICRF wave used for heating also remains high in the outer region. From the viewpoint of the axial transport of high-energy ions due to the low-frequency fluctuations, clarification of the properties of these nonlinearly generated waves is needed and will be addressed in future studies. An understanding of the nonlinear coupling among ICRF waves, including AIC waves, will lead to the production of higher-beta plasma in a mirror field and will also be useful for applications such as high-power space propulsion systems using radiofrequency plasma.

The authors would like to thank Professor A. Mase for useful discussions. This work was partly supported by Grants-in-Aid for Scientific Research from JSPS, Japan (Nos. 25400531 and 15K17797) and by the Bidirectional Collaborative Research Program of the National Institute for Fusion Science, Japan (NIFS14KUGM097 and NIFS14KUGM086).

[1]D. F. Escande, P. Martin, S. Ortolani, A. Buffa, P. Franz, L. Marrelli, E. Martines, G. Spizzo, S. Cappello, A. Murari, R. Pasqualotto, and P. Zanca, Phys. Rev. Lett. **85**, 1662 (2000).
[2]R. Lorenzini, E. Martines, P. Piovesan, D. Terranova, P. Zanca, M. Zuin, A. Alfier, D. Bonfiglio, F. Bonomo, A. Canton *et al.*, Nat. Phys. **5**, 570 (2009).
[3]M. Yamada, R. Kulsrud, and H. Ji, Rev. Mod. Phys. **82**, 603 (2010).

[4]P. H. Diamond, S.-I. Itoh, K. Itoh, and T. S. Hahm, Plasma Phys. Controlled Fusion **47**, R35 (2005).
[5]A. Fujisawa, Nucl. Fusion **49**, 013001 (2009).
[6]M. Porkolab and R. Chang, Rev. Mod. Phys. **50**, 745 (1978).
[7]S. G. Baek, R. R. Parker, S. Shiraiwa, G. M. Wallace, P. T. Bonoli, M. Porkolab, Y. Takase, D. Brunner, I. C. Faust, A. E. Hubbard, B. LaBombard, and C. Lau, Phys. Plasmas **21**, 061511 (2014).
[8]M. Inutake, T. Cho, M. Ichimura, K. Ishii, A. Itakura, I. Katanuma, Y. Kiwamoto, Y. Kusama, A. Mase, S. Miyoshi, Y. Nakashima, T. Saito, A. Sakasai, K. Sawada, I. Wakaida, N. Yamaguchi, and K. Yatsu, Phys. Rev. Lett. **55**, 939 (1985).
[9]T. Tamano, Phys. Plasmas **2**, 2321 (1995).
[10]M. Ichimura, M. Inutake, R. Katsumata, N. Hino, H. Hojo, K. Ishii, T. Tamano, and S. Miyoshi, Phys. Rev. Lett. **70**, 2734 (1993).
[11]R. Ikezoe, M. Ichimura, M. Hirata, T. Iwai, T. Yokoyama, Y. Ugajin, T. Sato, T. Iimura, Y. Saito, M. Yoshikawa, J. Kohagura, Y. Shima, and T. Imai, Nucl. Fusion **53**, 073040 (2013).
[12]M. Ichimura, H. Hojo, K. Ishii, A. Mase, Y. Nakashima, T. Saito, T. Tamano, and K. Yatsu, Nucl. Fusion **39**, 1995 (1999).
[13]M. Inutake, M. Ichimura, H. Hojo, Y. Kimura, R. Katsumata, S. Adachi, Y. Nakashima, A. Itakura, A. Mase, and S. Miyoshi, Phys. Rev. Lett. **65**, 3397 (1990).
[14]M. Ichimura, M. Inutake, S. Adachi, D. Sato, F. Tsuboi, Y. Nakashima, I. Katanuma, A. Itakura, A. Mase, and S. Miyoshi, Nucl. Fusion **28**, 799 (1988).
[15]R. Ikezoe, M. Ichimura, M. Hirata, T. Yokoyama, Y. Iwamoto, T. Okada, S. Sumida, K. Takeyama, S. Jang, T. Oi, K. Ichimura, and Y. Nakashima, Fusion Sci. Technol. **68**, 63 (2015).
[16]N. Bretz, Phys. Fluids B **4**, 2414 (1992).
[17]A. Mase, M. Ichimura, H. Satake, R. Katsumata, T. Tokuzawa, Y. Ito, H. Hojo, E. J. Doyle, A. Inutake, and T. Tamano, Phys. Fluids B **5**, 1677 (1993).
[18]A. Mase, M. Kobayashi, N. Oyama, T. Tokuzawa, H. Inutake, M. Yokoi, A. Itakura, H. Hojo, L. G. Bruskin, M. Ichimura, and T. Tamano, Fusion Eng. Des. **34–35**, 371 (1997).
[19]J. H. Lee, W. A. Peebles, E. F. Jaeger, E. J. Doyle, N. C. Luhmann, Jr., C. C. Petty, R. I. Pinsker, R. Prater, and T. L. Rhodes, Phys. Rev. Lett. **80**, 2330 (1998).
[20]E. Mazzucato, Rev. Sci. Instrum. **69**, 2201 (1998).
[21]R. Nazikian, G. J. Kramer, and E. Valeo, Phys. Plasmas **8**, 1840 (2001).
[22]L. G. Bruskin, A. Mase, N. Oyama, K. Shinohara, and Y. Miura, Plasma Phys. Controlled Fusion **45**, 1227 (2003).
[23]A. Krämer-Flecken, V. Dreval, S. Soldatov, A. Rogister, V. Vershkov, and the TEXTOR-Team, Nucl. Fusion **44**, 1143 (2004).
[24]J. B. Wilgen, P. M. Ryan, G. R. Hanson, D. W. Swain, S. I. Bernabei, N. Greenough, S. DePasquale, C. K. Phillips, J. C. Hosea, and J. R. Wilson, Rev. Sci. Instrum. **77**, 10E933 (2006).
[25]T. Yamada, A. Ejiri, Y. Shimada, T. Oosako, J. Tsujimura, Y. Takase, and H. Kasahara, Rev. Sci. Instrum. **78**, 083502 (2007).
[26]A. Ejiri, T. Yamada, Y. Adachi, O. Watanabe, and Y. Takase, Plasma Phys. Controlled Fusion **50**, 065003 (2008).
[27]S. Shiraiwa, S. Baek, A. Dominguez, E. Marmar, R. Parker, and G. J. Kramer, Rev. Sci. Instrum. **81**, 10D936 (2010).
[28]H. Hojo, A. Mase, R. Katsumata, M. Inutake, A. Itakura, and M. Ichimura, Jpn. J. Appl. Phys., Part 1 **32**, 3287 (1993).
[29]H. Hojo and A. Mase, J. Plasma Fusion Res. **69**, 1043 (1993).
[30]Y. Yamaguchi, M. Ichimura, H. Higaki, S. Kakimoto, K. Nakagome, K. Nemoto, M. Katano, H. Nakajima, A. Fukuyama, and T. Cho, Plasma Phys. Control. Fusion **48**, 1155 (2006).
[31]M. Ichimura, Y. Yamaguchi, Y. Motegi, H. Muro, T. Ouchi, S. Sato, T. Murakami, Y. Sekihara, and T. Imai, J. Plasma Fusion Res. SERIES **8**, 893 (2009).
[32]Y. C. Kim and E. J. Powers, IEEE Trans. Plasma Sci. **7**, 120 (1979).
[33]Ch. P. Ritz and E. J. Powers, Physica D **20**, 320 (1986).